INTERNATIONAL JOURNAL OF PRECISION ENGINEERING AND MANUFACTURING Vol. 17, No. 4, pp. 511-515 APRIL 2016 / 511
DOI: 10.1007/s12541-016-0064-2 ISSN 2234-7593 (Print) / ISSN 2005-4602 (Online)

An Optimal Study of Wind Measurement Device using Piezoelectric Unimorph Benders

HongSeok Jang[1], YoungTaek Cha[1], HongSeok Lee[1], SungJoon Choi[1,#], and Jongkyu Park[2]

1 Korea Institute of Industrial Technology, 2/F Choi John's Hall, 13-13, Hayang-ro, Hayang-eup, Gyeongsan-si, Gyeongsangbuk-do, 38430, South Korea
2 Department of Mechanical Engineering, Changwon National University, 20, Changwondaehak-ro, Uichang-gu, Changwon-si, Gyeongsangnam-do, 51140, South Korea
Corresponding Author / E-mail: sjchoi@kitech.re.kr, TEL: +82-53-607-1101, FAX: +82-53-607-1120

KEYWORDS: Anemovane, Piezoelectric unimorph bender, Transducer, Multi-physics analysis

A piezoelectric unimorph anemovane is proposed and analyzed for measuring precisely variation of wind direction and speed. The proposed anemovane has various advantages, compared with general anemovane. It can detect the wind in all direction, and be fabricated as small one. This anemovane was designed as the shape similar to a sea urchin. We use cantilevers to imitate prickles projected on the sea urchin sphere. If the wind blows, it hit the cantilever and the pressure makes the voltage signal through the piezoelectric unimorph bender. The simulation of the proposed system was performed using the FEM software (COMSOL Multi-physics), and the multi-physics analysis (Fluid mechanics, Mechanics and Electrostatics) was executed by considering real boundary conditions. Based on FEM analysis of the new anemovane with the new structure and control method, the characteristics between the fluid and the piezoelectric unimorph bender was comprehended. The possibility of the proposed anemovane was verified through the fabrication and the experiment.

Manuscript received: April 15, 2015 / Revised: October 29, 2015 / Accepted: December 10, 2015
This paper was presented at ISGMA 2015

1. Introduction

Meteorological observations of weather in modern life, has had a significant impact on all sectors of society and everyday life. Meteorological observation differs from the observation of other natural phenomena. Because the weather always changes, temporal and spatial elements should be considered. By measuring pressure, humidity, wind speed in real time from each location, and understanding the state of the atmosphere, accurate weather observation is possible.

Recently, anemovanes of various forms have been developed for measuring the change of the wind, which is one of the core elements of the meteorological observation. As a general anemovane, there is a rotating anemovane, thermal field variable anemovane, and ultrasonic anemovane.[1-3] These anemovane have the demerits that it has the slow response ability and the limited measuring range. Furthermore, the wind velocity and direction should be measured separately. Specifically, new systems have been developed for improving the existing anemovane. In the research using MEMS (Micro electro Mechanical Systems), there are a anemovane using the cantilever sensor, a anemovane of thermal sensing type, a anemovane using thermal flow sensor, and so on.[4-6] In the case using piezoelectric effect, there are anemovane using the ultrasonic wave or the displacement of the piezoceramic and so on.[7-9]

Accordingly, in this research, a new 3-dimensional measurement system was proposed using the piezoelectric unimorph bender with fast response characteristics.[10] The proposed anemovane have the shape similar to a sea urchin. It consist the many cantilever and the body of sphere shape. The cantilever is piezoelectric unimorph bender for sensing the wind, and is composed of the lamination structure of piezoelectric material and stainless steel. When the flow of the generated air in the atmosphere propagates on the piezoelectric unimorph bender, the wind pressure is generated between the air and the piezoelectric unimorph bender. The pressure makes the voltage signal through the piezoelectric unimorph bender. By analyzing the output values in each location, the wind velocity and direction can be decided. In this paper, the theoretical prediction model composed of the design parameters of the piezoelectric unimoph bender, was considered, and then the tendency of the theoretical prediction was confirmed by using the multi-physics simulation. Finally the application feasibility of this system was verified through experiments in the real environment.

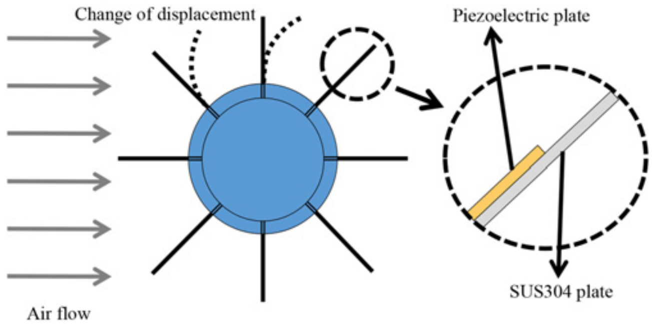

Fig. 1 The schematic diagram of proposed anemovane system

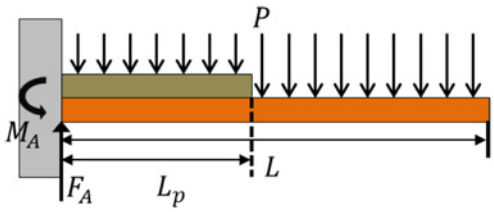

Fig. 2 The schematic diagram of the piezoelectric unimorph bender

2. Theory

In this research, the piezoelectric bender constitutive relation should be applied for optimal design because the shape of the cantilever sensor is unimorphic. That is, the piezoelectric material constitutive relation can be written using Voigt notation as follows:

$$\begin{aligned} S_1 &= s_{11}^E T_1 + d_{13} E_3 \\ D_3 &= d_{31} T_1 + \varepsilon_{33}^T E_3 \end{aligned} \tag{1}$$

These equations are transformed into the relation between force-like variables and displacement-like variables by applying several assumptions and boundary conditions. The unimorphic piezoelectric equations are follows.[11] In this equation, the external pressure by the wind is assumed to be equal to the equivalent force over the cantilever surface area.

$$\begin{bmatrix} \delta \\ q \end{bmatrix} = \begin{bmatrix} a_{11}A & a_{12} \\ a_{12}A & a_{22} \end{bmatrix} \begin{bmatrix} p \\ V \end{bmatrix} \tag{2}$$

$$a_{11} = \frac{2 s_m L^3}{w t_m^2} \cdot \frac{[2\eta^2\xi^4 + \{11\eta\xi^3 - 9\lambda_1(3 - 3\lambda_1 + \lambda_1^2)\eta\xi^3 + 18(1-\lambda_1)^3\eta\xi^2 + 12(1-\lambda_1)^3\eta\xi + 3(1-\lambda_1)^3\}]}{\eta^2\xi^4 + 4\eta\xi^3 + 6\eta\xi^2 + 4\eta\xi + 1} \tag{3}$$

$$a_{12} = a_{21} = \frac{3d \cdot L^2}{t_m^2} \cdot \frac{(2-\lambda_1)\lambda_1\eta\xi^3(1+\xi)}{\eta^2\xi^4 + 4\eta\xi^3 + 6\eta\xi^2 + 4\eta\xi + 1} \tag{4}$$

$$a_{22} = \frac{L w \varepsilon_{33}^T}{t_p} \cdot \lambda_1 \left(1 - \frac{k^2\eta\xi(1+\xi)}{\eta^2\xi^4 + 4\eta\xi^3 + 6\eta\xi^2 + 4\eta\xi + 1} \right) \tag{5}$$

Where,

$\xi = \frac{t_m}{t_p}$ Thickness ratio (Elastic layer over piezoelectric layer)

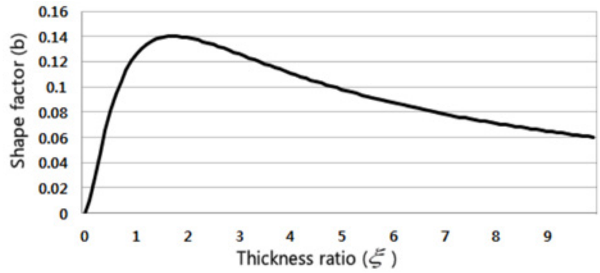

Fig. 3 The shape factor according to thickness ratio of the SUS304 and PZT

$\eta = \frac{s_p}{s_m} = \frac{E_m}{E_p}$ Compliance (Young's modulus) ratio

$k^2 = \frac{d_{31}^2}{\varepsilon_{33}^T s_p}$ Electromechanical coupling factor

$\lambda_1 = \frac{L_p}{L}$ Length ratio (Piezoelectric layer length over Elastic layer length)

These equations should be modified for sensor applications. That is, internal variables are voltage and displacement.

$$\begin{bmatrix} \delta \\ V \end{bmatrix} = \begin{bmatrix} a_{11}A + \frac{(a_{12}A)^2}{a_{22}} & -\frac{1}{a_{12}A} \\ \frac{a_{12}A}{a_{22}} & -\frac{1}{a_{22}} \end{bmatrix} \begin{bmatrix} p \\ q \end{bmatrix} \tag{6}$$

If open circuit is assumed as q=0, output terminal voltage is derived as follows

$$\begin{aligned} V &= \frac{a_{12}}{a_{22}} A p \\ &= \left(\frac{3d \cdot L}{w \varepsilon_{33}^T t_m} \cdot \frac{(2-\lambda_1)\eta\xi^2(1+\xi)}{\eta^2\xi^4 + 4\eta\xi^3 + 6\eta\xi^2 + 4\eta\xi + 1 - k^2\eta\xi(1+\eta\xi^3)} A p \right) \end{aligned} \tag{7}$$

In this equation, design parameters are length ratio, thickness ratio, and compliance ratio between piezoelectric layer and elastic layer. That is, if the sensor is analyzed theoretically, length ratio should be small in order to increase output voltage. Additionally, if material constant is fixed, following equation is expressed with shape factor for optimal design.

$$\begin{aligned} b &= \frac{V}{Ap} \left(\frac{w \varepsilon_{33}^T t_m}{3d \cdot L(2-\lambda_1)} \right) \\ &= \frac{\eta\xi^2(1+\xi)}{\eta^2\xi^4 + 4\eta\xi^3 + 6\eta\xi^2 + 4\eta\xi + 1 - k^2\eta\xi(1+\eta\xi^3)} \end{aligned} \tag{8}$$

If k2 is assumed as 0.137 in PZT and η is assumed as 1.6 in SUS304, Fig. 3 is plotted. Therefore, the thickness of the piezoelectric should be designed thin than SUS304. Also, as shown in the formula mentioned above, the length of the piezoelectric should be short than SUS304.

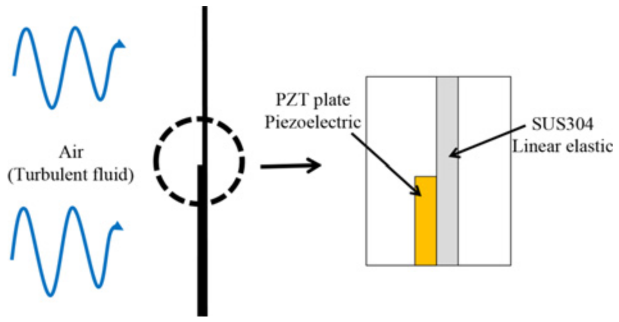

Fig. 4 Multi-physical model of the proposed anemovane

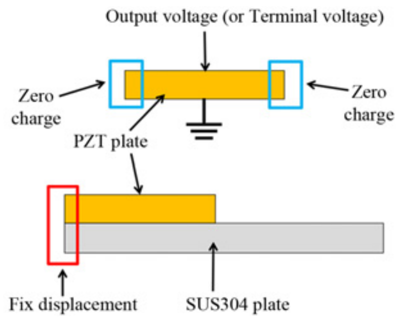

Fig. 5 Boundary conditions of PZT and SUS

Table 1 The simulation step

(mm)	PZT Thickness	PZT Length	PZT Width	SUS304 Thickness	SUS304 Length	SUS304 Width
Step 1	0.15	Sweep Analysis	10	0.15	40	10
Step 2	0.15	Result of 1 Step	10	0.15	Sweep Analysis	10
Step 3	Sweep Analysis	Result of 1 Step	10	Sweep Analysis	40	10
Step 4	0.15	Result of 1 Step	Sweep Analysis	0.15	40	Sweep Analysis

3. The Multi-Physics Simulation

3.1 Multi-physical model of the piezoelectric unimorph

The simulation of the proposed system was performed using COMSOL Multi-physics. Fig. 4 shows the multi-physical model of the proposed system on finite element method. The multi-physics model consists of the piezoelectric, SUS304 (Stainless Use steel) and the turbulent fluids. In order to output the electrical signals, the piezoelectric module is used. To assume the atmospheric air, turbulent condition was applied. This multi-physical model is a combination of the piezoelectric, structural, and fluid phenomenon, where each physical quantity is coupled at its boundaries. For example, when the wind blows, it hits the piezoelectric unimorph. At this point, the pressure is generated according to the area of PZT-SUS304. The structural deformation of PZT-SUS304 is generated by the pressure and the output voltage is generated from the PZT.[12]

The flow of the air is modeled as the turbulent fluid based on the Reynolds number (Re). In order to model the interaction between flow medium and structure, the boundaries of PZT-SUS304 contacted with air are loaded as the wind pressure. The boundary conditions of the PZT plate and the SUS304 plate are as shown in Fig. 5. SUS304 diaphragm is assume to be linear elastic model; hence the fixed displacement condition is applied to the one end side of SUS304 plate while the free displacement condition is applied to top and bottom of the Si diaphragm. The top of PZT plate is connected into the output voltage terminal for measuring the value according to pressure and displacement, and the bottom of PZT unimorph is grounded. Additionally, the zero charge conditions are applied to two sides of the PZT diaphragm because any charge does not exist at the sides of PZT diaphragm in the ideal model.

3.2 Analysis of multi-physical simulation

The static analysis was performed for understanding the tendency on the theory, and fix condition, wind velocity was applied 1 m/s and wind direction was applied only the forward direction at 1 atm. The simulation was performed as shown in Table 1 and the simulation results are shown in Fig. 6. The sweep analysis step 1 and step 2, was performed depending on the length of PZT and SUS304. When the PZT length is short, the output values are increased. But, the PZT length has the maximum value at a particular length; 4 mm. When the SUS304 length is long, the output values are increased. It means that the stress is increased in the PZT, because of the increased wind pressure according to the area of the SUS. At the step 1 and step 2, The PZT length of the maximum output voltage was applied to the step 3. In the case of SUS304, there is no particular value. So, the first SUS304 length was applied to the step 3. The sweep analysis of step 3 was performed depending on the thickness of PZT and SUS304. When the PZT thickness was thicker than the SUS304 thickness, the output value is increased. But when the PZT thickness was increased over the particular value; 0.15 mm, the output value is decreased. It means that the generated stress have not an effect on the increased PZT thickness. The sweep analysis of step 4 was performed the width of PZT and SUS304 at the same time. When the width was increased, the output values are high. But, when considering the three-dimensional shapes of the entire system, the width should not be too wide.

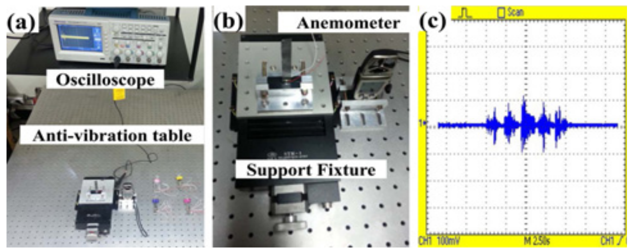

Fig. 6 Experiment equipment and output signal

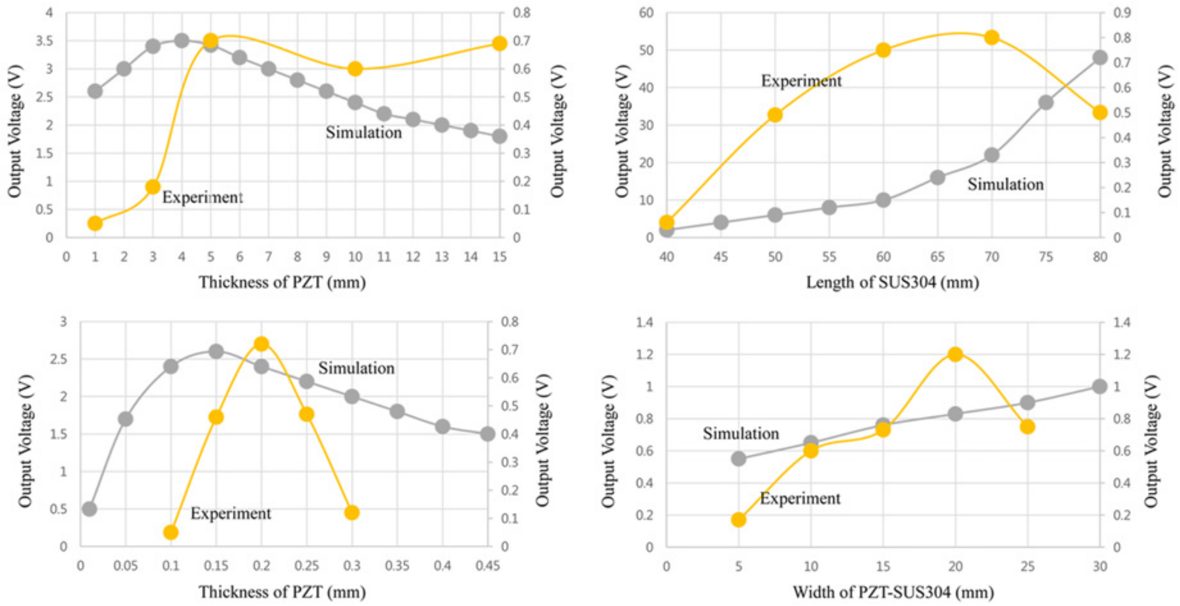

Fig. 7 Result of simulation and experiment

4. Experiment

Fig. 6 shows the experiment equipment for confirming the interaction of the fluid and the piezoelectric unimorph bender. The piezoelectric unimorph bender was fabricated as the same dimension with the simulation. In order to measure the output voltage, the oscilloscope was used. Also, the anti-vibration table was used to prevent from the external vibrations other than the wind. Also, the air-gun was used for generating the momentary wind and the anemometer for measuring the wind velocity. The one end of bender should be fixed as shown in the simulation. But, the fabricated piezoelectric unimorph bender can't be fixed bonding only because of thin thickness. So, the piezoelectric unimorph bender was fabricated longer than real size and this part was fixed using support fixture. As the experiment procedure, the anemometer set beside the support fixtures, the average velocity by the air gun is controlled, and the wind is sprayed to the piezoelectric unimorph bender. In this way, the experiment was performed as the same procedure with the simulation from the step 1 to the step 4. The five specimens were fabricated for each step. As shown in Fig 6(c), the output signal was measured by constant cycle. Then the maximum output values for each cycle was calculated and recorded by the average value. As shown in Fig. 7, the comparison between the experimental results and simulation shows analogous patter, but there is a difference at step 4 and step 2. Its origin is expected that it was static analysis and damping effect was neglected. In the case of step 2, when the length of SUS304 is increased, the vibration was often generated. At this time, it is expected that the stress by wind pressure was decreased.

5. Conclusion

In this paper, a new anemovane with the piezoelectric unimorph bender was proposed for measuring the wind velocity and 3-dimensional wind direction. And the application feasibility of this system was verified through experiment. The design parameter following the theory was selected, and the sweep analysis was performed. In the experimental results, the output voltage was generated greater than the simulation. The reason for this is expected that the damping effect was not applied to the simulation and the characteristics with respect to the time didn't be considered. Another reason is that the difference in the fixing method of the simulation and the real specimen. But, it could be check that the comparison graph between the simulation and the experiment had the similar tendency. In the future, the study which improves the sensitivity will be performed through the optimal design and the material analysis.

REFERENCES

1. Park, S. K. and Han, D. W., "Anemometer and Measuring Method of Wind Velocity using Ultrasonic," KR Patent, No. 10-2012-0087602, 2011.

2. Jo, N. K. and Lee, D. H., "Anemovane," KR Patent, No. 10-2011-0125504, 2011.

3. Yun, C. I., Lee, M. Y., and Kwon, W. C., "Anemoscope and Anemometer," KR Patent, No. 2003-0044501, 2003.

4. Zyłka, P., Modrzyñski, P., and Janus, P., "Vortex Anemometer using Mems Cantilever Sensor," Journal of Microelectromechanical Systems, Vol. 19, No. 6, pp. 1485-1489, 2010.

5. Yoo, E. S., Shin, K. S, Cho, N. K., Park, J. H., and Lee, D. S., "A Micro Wind Sensor Fabricated using MEMS Technology," Proc. of KIEE Conference, pp. 1468-1469, 2008.

6. Piotto, M., Pennelli, G., and Bruschi, P., "Fabrication and Characterization of a Directional Anemometer based on a Single Chip MEMS Flow Sensor," Microelectronic Engineering, Vol. 88, No. 8, pp. 2214-2217, 2011.

7. Han, D., Kim, S., and Park, S., "Two-Dimensional Ultrasonic Anemometer using the Directivity Angle of an Ultrasonic Sensor," Microelectronics Journal, Vol. 39, No. 10, pp. 1195-1199, 2008.

8. Nakai, T. and Shimoyama, K., "Ultrasonic Anemometer Angle of Attack Errors under Turbulent Conditions," Agricultural and Forest Meteorology, Vols. 162-163, pp. 14-26, 2012.

9. Gong, B. G., "The Developement of a Wind Direction/Speed Measurement Equipment using RTD and Piezo Sensors," M.Sc. Thesis, Department of Electrical Engineering, Changwon National University, 2012.

10. Jang, H., Na, Y., Park, J., and Choi, S., "Design and Multi-Physics Analysis of Anemovane using the Piezoelectric Unimorph," Ferroelectrics, Vol. 452, No. 1, pp. 114-121, 2013.

11. Park, J.-K. and Moon, W.-K., "Constitutive Relations for Piezoelectric Benders under Various Boundary Conditions," Sensors and Actuators A: Physical, Vol. 117, No. 1, pp. 159-167, 2005.

12. Kim, C. and Shin, J.-W., "Topology Optimization of Piezoelectric Materials and Application to the Cantilever Beams for Vibration Energy Harvesting," Int. J. Precis. Eng. Manuf., Vol. 14, No. 11, pp. 1925-1931, 2013.